A Morphological Study of Well-Defined Smectic Side-Chain LC Block Copolymers

Mitchell Anthamatten, Wen Yue Zheng, and Paula T. Hammond*

Department of Chemical Engineering, Massachusetts Institute of Technology, 77 Massachusetts Av, Rm 66-550, Cambridge, Massachusetts 02139-4307

Received March 2, 1999; Revised Manuscript Received May 18, 1999

ABSTRACT: The influence of smectic level ordering on domain morphology has been studied in a series of monodisperse side-chain liquid-crystalline (LC) diblock copolymers. These systems, which consist of a polystyrene-*b*-methacrylate-based side-chain LC, were investigated using electron microscopy and room temperature X-ray scattering. A morphological phase diagram based on volume fraction and molecular weight has been determined for molecular weights up to 40 000 Da. A broad lamellar regime was identified that extends to unusually low LC compositions. At intermediate LC volume fractions around 0.48−0.56, morphologies were predominately lamellar but included many transitional defects in the form of modified layer or hexagonal perforated layer morphologies. The formation of large domains and focal−conic superstructures is shown to depend on the length of the PS block and the overall molecular weight. Samples of lamellar and cylindrical morphologies were oriented using roll casting from solvent and fiber drawing. SAXS diffractograms of oriented samples indicated that in roll-cast films of the copolymer with a hexyl spacer smectic layers were oriented perpendicular to the lamellar morphology, but the longer decyl spacer system resulted in orientation of the smectic layers parallel to the lamellae. These results imply that the degree of decoupling of the mesogen from the backbone is critical to LC orientation within the layers.

Introduction

Ferroelectric liquid crystals have been of interest for the past two decades because of their fast response times and bistable switching capabilities. The exhibition of these properties relies on application of an electric or magnetic field, or the use of surface treatments, to untwist the helical smectic C* phase and induce macroscopic polarization. Applications of these materials are hindered by two major problems—maintaining constant cell thicknesses and controlling the orientation of the smectic C* mesogens throughout the electrooptical cell. Phase segregated liquid crystalline diblock copolymers offer promise in overcoming both of these obstacles. The glassy, non-liquid-crystalline block provides structural integrity, enabling the fabrication of free-standing films or uniform coatings. The block copolymer structure results in microphase segregation of the glassy and LC domains. It is anticipated, and has been illustrated, that the morphological interface between these domains can stabilize the liquid-crystal side-chain mesogens, just as a buffed surface in an electrooptical cell stabilizes a low molar mass liquid crystal.[1,2] The interaction at the interface must be strong enough for mesogenic orientation to subsist for sufficient depths but weak enough so that mesogens can be reoriented with electric or magnetic fields. A number of groups have reported the development of side-chain liquid-crystalline block copolymers[3−8] including ferroelectric LC block copolymers.[9−11] However, the overlap of morphological and liquid-crystalline orders is far from understood, and the key to the refinement and design of new materials is further knowledge on mesogenic behavior at a block copolymer interface.

Recently, we reported the synthesis and phase behavior of a new series of ferroelectric side-chain liquid-crystalline block copolymers.[12] These microphase segregated block copolymers exhibit smectic mesophases over broad temperature ranges.[13] It was found that the block copolymer interface effectively stabilizes the chiral smectic C* phase. There are also indications that the presence of the liquid-crystalline phase influences microphase segregation; in a previous paper,[13] this was illustrated for the first time by the introduction of the order−disorder transition at the liquid-crystalline clearing point.

In this paper, the room temperature morphology of these side-chain liquid-crystalline block copolymers, and the influence of the liquid-crystalline phase on that morphology, is examined. Block copolymer phase diagrams will be discussed for a broad range of polymers as a function of liquid-crystalline content and molecular weight. Specific characteristics will be discussed, including the breadth of the lamellar regime and the apparent absence of LC cylinders, as well as transitional morphological defects appearing at unusually low LC volume fractions. The effects of morphological orientation on the arrangement of the liquid-crystalline smectic layers within the block copolymer domains will be addressed, including a further investigation of issues raised in an earlier communication[2] regarding the unusual parallel arrangement of smectic layers within a lamellar block copolymer domain.

Experimental Section

Materials. All block copolymers were synthesized using direct anionic polymerization of styrene followed by polymerization of a mesogenic methacrylate monomer to obtain diblock copolymers. Details of the synthesis are described elsewhere.[8,14]

Sample Preparation. *Solvent-Cast Films*: Thin films were slowly cast from 3 wt % solution in toluene or tetrahydrofuran and dried in a vacuum for 2 days to remove remaining solvent. The films were then annealed at 110 °C for 2 days before SAXS measurements or sample preparation for TEM.

Roll-Cast Films: Oriented samples were prepared by roll-casting from 25 wt % solution in toluene. During the roll-

10.1021/ma9903153 CCC: $18.00
Published on Web 07/02/1999

Table 1. Molecular Weight, Composition, and Morphological Characteristics of PS−*n*BPB Block Copolymers

	M_n (kg/mol)			morphology domain size (Å)[a]		
diblock	PS block	LCblock	p_i	SAXS	TEM	morphology[b]
			Hexyl Series			
PS−HBPB12	48.1	4.8	1.08	*c*	*c*	DP
PS−HBPB20	21.8	5.3	1.11	*c*	*c*	DP
PS−HBPB24	40.3	7.7	1.12	*c*	*c*	DP
PS−HBPB32	17.7	7.3	1.07	186 (90)	210	LAM
PS−HBPB41	11.0	7.3	1.06	173 (85, 56, 42)	140	LAM
PS−HBPB43	10.3	7.4	1.08	153 (75)	140	LAM
PS−HBPB50	8.4	11.0	1.14	143, 175		LAM, HPL
PS−HBPB51	6.8	7.7	1.07	112 (56,37), 170 (98, 85, 64)	120	LAM, HPL
PS−HBPB54	14.9	17.5	1.19	178 (83)	150	LAM
PS−HBPB56	10.5	11.0	1.07	146 (71), 190, 216		LAM, (HPL or ML)
PS−HBPB58	8.8	12.0	1.11	123 (59), 156 (77, 52)		LAM, ML
PS−HBPB79	4.8	16.3	1.08	130 (75, 65, 49)	120	HPC
PMHBPB		7.0	1.10			
			Decyl Series			
PS−DBPB37	14.3	8.3	1.09	191 (94, 63)	220	LAM
PS−DBPB40	18.5	12.0	1.24	203 (101, 68)		LAM
PS−DBPB49	10.3	8.7	1.11	151 (76)	150	LAM
PS−DBPB57	8.1	9.4	1.13	145 (70, 46)		LAM
PS−DBPB59	11.7	17.2	1.06	140	140	LAM/HPL[d]
PS−DBPB63	5.7	8.7	1.09	127 (64)	140	LAM/HPL[d]
PMDBPB		8.3	1.10			

[a] The morphological domain size and type were determined using a combination of SAXS and TEM. Morphological *d* spacings that correspond to first-order SAXS reflections are reported with higher-order reflections listed in parentheses. [b] DP = dispersed phase, LAM = lamellae, ML = modified layer, HPL = hexagonal perforated layer, HPC = hexgonally-packed cylinders. [c] Lack of discernible SAXS peaks with ill-defined morphology. [d] Metastable features disappear on fiber-drawing and roll-casting.

casting process, a block copolymer solution is processed between rotating cylinders, while at the same time the solvent is evaporated at a controlled rate. As the solvent evaporates, the polymer concentration increases, and the block copolymer microphase-segregates into a globally oriented microstructure. Detailed information on the experimental aspects of roll-casting is available.[15,16]

Fibers: The polymer was placed on a Teflon-coated surface and heated well above its glass transition temperature (∼180 °C). Individual fibers were drawn from the polymer melt using a metal probe. Fibers were quenched to a brittle state as they were drawn. The hardened fibers were sectioned into 1−2 cm segments for X-ray experiments. The fiber thickness ranged from 50 to 200 μm.

Characterization. A Waters gel permeation chromatograph with a 440 nm UV absorption detector and R401 differential refractometer was used to determine the molecular weights of the polymers; tetrahydrofuran and toluene were used as the mobile phases at 1.0 mL/min, and the Waters polystyrene gel columns were calibrated with monodisperse polystyrene standards.

Polarizing optical microscopy was done using a Leitz optical microscope with CCD camera attachment and Mettler FP-82 hot stage and controller (heating/cooling rate of 10 °C/min).

Transmission electron microscopy (TEM) thin sections (40−60 nm) were prepared by cutting a small piece of thin film embedded in epoxy resin on a Reichert-Jung FC4E Ultracut E microtome equipped with a diamond knife. The sections were collected on copper grids and were stained in RuO_4 vapor for 30 min to make enough phase contrast for TEM observation. The TEM morphology studies were carried out using a JEOL 200CX electron microscope in bright field mode operated at accelerating voltages of 160−200 kV.

Small-angle X-ray (SAXS) scattering was conducted using a Rigaku RU-H3R rotating anode gererator producing Cu Kα radiation (λ = 1.54 Å) at 40 kV and 30 mA. A two-dimensional GADDS/HI-STAR area detector manufactured by Siemens containing an array of 512 × 512 wires was used to collect data. All experiments were carried out in an evacuated flight path at a sample-to-detector distance of 63.8 cm which enabled the resolution of *d* spacings in the range 20−450 Å.

Scheme 1. Molecular Structure of PS−*n*BPB Diblock Copolymer

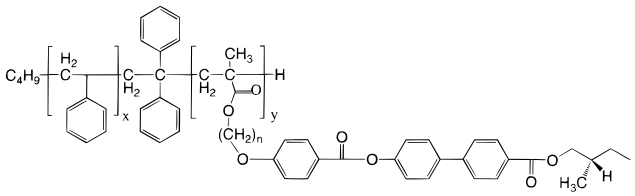

Results and Discussion

Morphologies and Phase Diagram of LC Diblocks. The block copolymers investigated in this study were synthesized using direct living anionic copolymerization of styrene with a mesogenic methacrylate based on a chiral biphenyl benzoate (BPB). The structure of the *n*BPB series of LC block copolymers is shown in Scheme 1.

The polymers consist of a glassy, amorphous, high-T_g polystyrene block and a side-chain LC methacrylate block with 100% substitution along the backbone. The glass transition temperatures of the LC blocks ranged from 25 to 40 °C in this series of materials. Two different alkyl spacer lengths were used to connect the mesogen to the polymer backbone—a hexyl (n = 6) spacer for the PS−HBPB series and a decyl (n = 10) spacer for the PS−DBPB series. A summary of the block copolymers synthesized and characterized is included in Table 1. Both high and low molecular weight polymers were examined, with a weight fraction of the LC block ranging from 12% to 79%. The block copolymers were monodisperse with polydispersity indexes ranging from 1.05 to 1.24.

SAXS *d* spacings and domain morphologies and spacings from TEM micrographs are summarized in Table 1. The spacer length was found to have some effect on the final morphology of the diblocks; therefore, two separate phase diagrams were developed on the basis of available data and are shown in Figure 1a for PS−

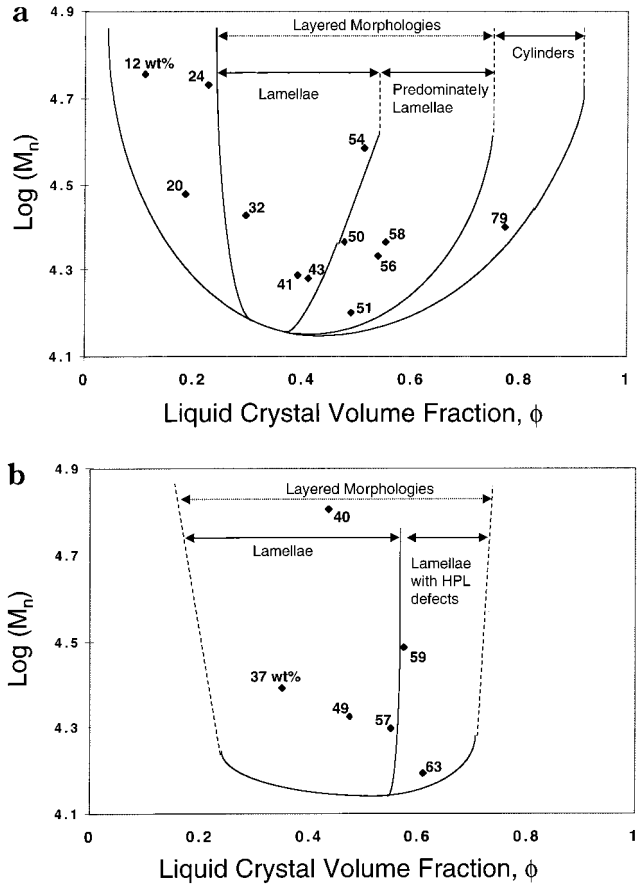

Figure 1. Morphological phase diagram for PS−*n*BPB diblock copolymers: (a) $n = 6$; (b) $n = 10$.

HBPB and Figure 1b for PS−DBPB systems. The lines of the phase diagrams were drawn to represent phase behavior on the basis of existing data and can be used to delineate general trends in the phase behavior of the PS−*n*BPB systems.

The phase diagrams in Figure 1 are based on the liquid-crystalline volume fraction of the diblocks ϕ_{LC}. This quantity can be obtained directly using liquid-crystal weight fractions from GPC measurements of the polymer before and after addition of the second block. The volume fraction is derived from weight fraction with the assumption that PS and LC homopolymers contribute ideally to the bulk density by

$$\hat{V}_{\text{diblock}} = \hat{V}_{LC} w_{LC} + \hat{V}_{PS} w_{PS} \qquad (1)$$

where $\hat{V}$ represents the molar volumes and w the weight fractions. This assumption was verified by carrying out density measurements of all homopolymers and diblocks using a flotation method similar to that used by Lednicky.[17] The homopolymer densities were 1.154 ± 0.003 and 1.126 ± 0.008 g/mL for PHBPB and PDBPB and 1.045 ± 0.01 g/mL for PS. The densities of the diblocks exhibited small negative deviations ($<-2.2\%$) from a linear extrapolation between homopolymer densities. This deviation may be due to the fact that some degree of mixing at the block copolymer interface may lower the effective packing of mesogens, thus lowering the copolymer density.

At low liquid-crystal volume fractions, for both the hexyl and decyl series, liquid-crystalline cylinders or spheres in a polystyrene matrix were not observed. Instead, an ill-defined morphology was observed at volume fractions of 23% and lower that was difficult to discern using TEM. The structures appear to be either density fluctuations due to spinodal decomposition or a disordered disperse phase similar to those observed by Hashimoto and others in solvent cast films of block copolymer/ homopolymer mixtures.[18] SAXS of films formed from this polymer do not exhibit clear peaks, which suggests poorly defined block copolymer interfaces or phase mixing. Although the PS−HBPB24 sample was very weakly birefringent, no smectic layers were observed using wide-angle X-ray scattering. This observation suggests the layered nature of the LC block has been destabilized in the disperse domains, leaving a nematic phase. At $\phi_{LC} = 11\%$ (PS−HBPB12) the block copolymer does not have any features visible in TEM or SAXS and exhibits only an isotropic phase.

The polymer morphology is lamellar at LC volume fractions as low as 30 wt %. The absence of LC cylinders in this range may be due to lowered stability of the smectic mesophase when confined to small cylindrical domains. A few other groups have identified morphologies with LC cylinders. Ober and Thomas have confirmed a phase containing smectic LC cylinders in a continuous matrix.[19] In their case, the polymer system was a polystyrene-*block*-1,2-polyisoprene copolymer system at a liquid-crystal volume fraction of 0.22, with cylinders of 190 Å and domain spacings of 760 Å. The stability of LC cylinders may well depend on the size of the cylindrical domains or the radius of curvature at the block copolymer interface relative to the size of the smectic layers. The domain *d* spacings of the methacrylate polymers discussed in this paper, and those of Fischer's,[20,21] are on the order of 140−200 Å, which are 3−4 times smaller than those described by Ober and Thomas. The limitations presented by increased curvature at the block copolymer interface may prevent the exhibition of smectic LC phases within small curved domains. However, observations in a recent investigation of cyanobiphenyl mesogenic side-chain LC diblocks by Yamada et al. counter this notion.[22] LC cylinders with domain sizes ~200−300 Å were reported for a high molecular weight diblock (36 kg/mol) with an unusually low LC fraction (53 wt %). On the basis of Figure 1, the corresponding microstructure for the PS−*n*BPB materials addressed in this paper would be a predominately lamellar morphology with indications of a continuous LC phase. In the Yamada paper, a TEM micrograph of the LC cylinder phase is shown in which OsO_4 stained dark regions are designated as LC regions; it is worth noting that we have consistently found the opposite contrast in TEM, in which the polystyrene blocks are the darker stained regions. Other issues such as tacticity, backbone flexibility, or the effective persistence length of the LC polymer chain may also play roles in determining the relative stability of layered phases. The diblocks in this study, as well as those of the Fischer and Watanabe groups, have a polymethacrylate backbone derived from anionic synthesis which usually results in a largely syndiotactic polymer.

As seen in Figure 1, both HBPB and DBPB phase diagrams exhibit broad lamellar regimes, resulting in asymmetrical morphological phase diagrams. The dominance of a layered structure is related to the fact that smectic liquid-crystalline phases share the same symmetry as lamellar phases. A number of the lamellar morphologies also indicated evidence of the presence of two or more morphologies within a given sample,

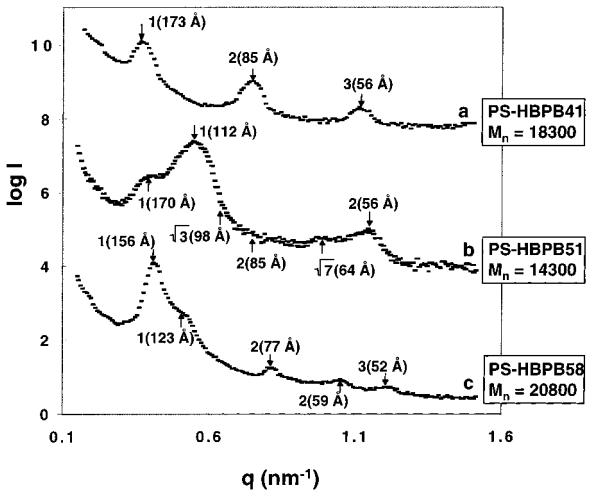

Figure 2. Saxs 1D line integrals of PS−HBPB diblock copolymers in lamellar−cylindrical transition regime: (a) PS−HBPB41, (b) PS−HBPB51, (c) PS−HBPB58. The SAXS data are plotted as the logarithm of the relative scattered intensity log $I(q)$ vs the scattering factor $q = 4\pi \sin \theta/\lambda$ where θ is one-half of the scattering angle and λ is the X-ray wavelength. The intensities of PS−HBPB41 and PS−HBPB51 have been multiplied by a factor of 10^3 and 10^7 to avoid overlap.

suggesting a transition region from a purely lamellar morphology to a continuous LC phase morphology. These systems exhibit modified layers (ML)[23] or hexagonal perforated layers (HPL),[24,25] such as those reported recently in fully amorphous block copolymers, as well as completely lamellar morphologies. The following samples in the hexyl series samples were identified to lie in this transition region: PS−HBPB50,51, 56,58 (ϕ_{LC} = 48, 49, 54, 55). Another sample in the same composition range, PS−HBPB54 (ϕ_{LC} = 52), would be expected to be included in this group on the basis of its liquid-crystalline content. However, this sample has a much higher molecular weight (M_n = 32 400, M_w = 38 400 g/mol) and was found to exhibit a pure lamellar morphology. This suggests the boundary between the transitional and lamellar region as drawn in Figure 1a. Figure 2 shows 1D SAXS line profiles of three solvent cast films from the hexyl series: (a) PS−HBPB41, (b) PS−HBPB51, and (c) PS−HBPB58. The 1:2:3:4 scattering pattern of the PS−HBPB41 film suggests a highly segregated lamellar morphology with a d spacing of 173 Å—this morphology was confirmed by TEM. With a slightly higher LC content and a lower molecular weight, the PS−HBPB51 pattern shows two first-order reflections corresponding to periodicities of 112 and 170 Å. Each first-order peak has a set of higher-order peaks that are difficult to assign due to convolution of the peaks and the structure factors. The 112 Å peak is stronger and broader than the 170 Å peak and has reflections corresponding to a scattering factor (q) ratio of 1:2:3, which indicates a lamellar morphology. The 170 Å peak exhibits higher-order reflections in the q signature pattern for hexagonal periodicity of $1:\sqrt{3}:\sqrt{7}$. The higher order reflections at $q = \sqrt{3}$ and 2 are nearly extinct and convolute with the tail of the first-order 116 Å peak; therefore, their intensities may be attenuated due to the structure factor. The intensities of the 112 Å reflections are an order of magnitude larger than the 170 Å reflections; thus, lamellar morphology is predominant. This observation is confirmed by TEM analysis. The SAXS pattern in Figure 2c of PS−HBPB58 also has two first-order peaks, again suggesting multiple morphologies. As seen in Figure 2c, higher-order reflections are distinct and correspond to a 1:2:3 pattern for both first-order peaks. PS−HBPB58 is thought to exhibit both lamellar and ML morphologies, each having a characteristic d spacing; modified layer morphologies consist of aligned cylinders forming layers, but lacking a specific hexagonal arrangement between cylinders. Similar multiple peaks were observed by Hajduk et al. in a study of polystyrene−isoprene block copolymers.[23] The differences between HPL and ML morphologies thus include the tendency toward hexagonal packing as found in the cylindrical phase. On observing the phase diagram, one notes that the PS−HBPB51 sample has a much lower molecular weight than PS−HBPB58 and is therefore closer to the transition to PS cylinders. The low molecular weight therefore may cause the onset of cylindrical morphologies, in the form of HPL, to be realized at lower LC volume fractions.

In the decyl series, defects common to the modified layer or hexagonal perforated layer are also observed at approximately 55 vol % LC block, such as those in the TEM images shown in Figure 3a,b for the 59 and 63 wt % polymers. The dark regions are polystyrene domains which are selectively stained with osmium tetroxide. These defects are found in solvent-cast films annealed for 2 or 3 days. These morphologies do not appear in polymer samples that are processed using a technique such as roll-casting or fiber-drawing, suggesting that the morphologies may be metastable or that kinetic effects are important to the observation of these phases. The defects indicate a transition from lamellar to cylindrical morphologies, as observed by other groups in studies of fully amorphous block copolymers.[23−25] Unlike the hexyl series, these transitional morphologies in the decyl series exhibit a single set of SAXS peaks. The d spacings between the two phases may be close in value for these samples, leading to convolution of the peaks, or the defects may be more sparsely distributed or arranged in a less periodic fashion.

In the hexyl series, as the liquid-crystal content is increased further, hexagonally packed polystyrene cylinders with a periodicity of 130 Å form in a continuous liquid-crystal matrix as indicated by the SAXS pattern shown in Figure 4 for PS−HBPB79. If a completely aligned hexagonal array of cylinders is assumed, the diameters of the cylinders and their intersticial spacing can be estimated. This calculation requires densities of the polystyrene and side-chain liquid-crystal domains. The calculation predicts the cylinders have radii of 32.5 Å with a spacing of 65 Å between them. This is enough space for about two layers of mesogens (~33 Å each) aligned end-to-end. A TEM image is shown in the inset of the figure and confirms the cylindrical morphology. The TEM data indicate d spacings of approximately 120 Å and PS cylinder diameters around 90−100 Å. These observations correspond to a LC volume fraction of 50%, which is much lower than the volume fraction calculated from the molecular weights and densities of each block (78%). Heck et al. has also observed unexpectedly large cylinders through TEM.[26] Several factors may contribute to the attenuated LC volume fraction observed through TEM. The RuO_4 stain molecules prefer polystyrene and may swell this phase. There may be a lower overall density near the cylinder interface, creating more permeable regions for the RuO_4 stain. This was illustrated in one study of an LC diblock copolymer,[27] in which the interface was preferentially stained rela-

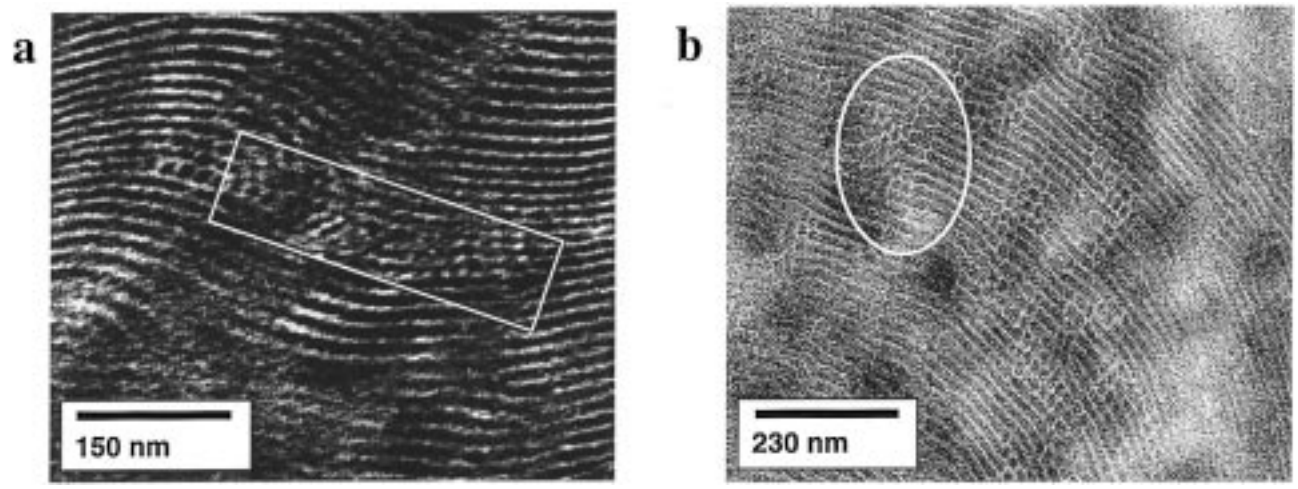

Figure 3. TEM micrographs of PS−DBPB diblock copolymers in lamellar−cylinder transitional regime: (a) PS−DBPB63, M_n = 14 400; (b) PS-DBPB59, M_n = 28 900. Dark regions represent the PS phase.

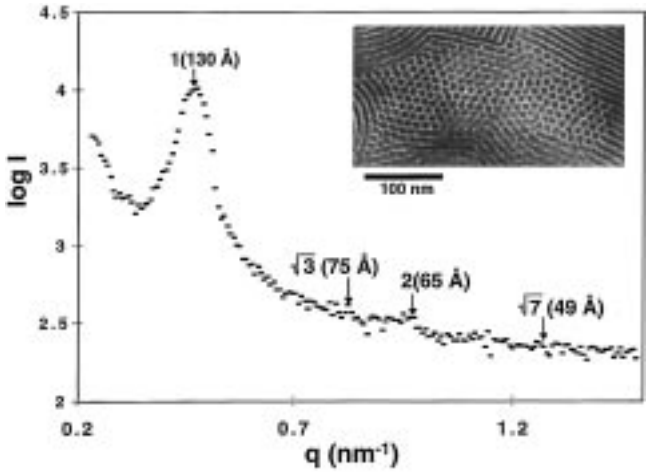

Figure 4. SAXS 1D line integral for PS−HBPB79. The inset is a TEM micrograph where dark regions indicate the PS domains.

tive to both bulk phases by using very short (5 min) staining times. Gido and Wang account for the disparity between calculated and TEM curvature by considering volume fractions, material characteristics, and molecular architecture.[28]

To summarize, composition versus molecular weight phase diagrams were constructed for both hexyl and decyl spacer lengths. For ϕ less than ~0.25, density fluctuations near the disorder transition or dispersed phase morphologies are present, consisting of poorly defined, nonperiodic arrays of LC spheres inside a continuous PS matrix. At higher LC fractions, a layered-morphology region exists which can be subdivided asymmetrically into purely lamellar morphologies (ϕ < 0.5) and predominately lamellar morphologies with cylindrical defects appearing with a ML or HPL signature (ϕ > 0.5). Finally, at high LC fractions, only hexagonal close-packed PS cylinders (HCP) are observed in a continuous LC phase.

Features of Lamellar Morphology as a Function of PS Block Length. The liquid-crystalline block length in a set of lower molecular weight block copolymers was kept constant while the polystyrene block length was systematically increased. For the hexyl series, the block copolymer morphology is shown in Figure 5 for three block copolymers with increasing polystyrene block length or decreasing liquid-crystal content. In all cases, the LC molecular weight is approximately 7000, corresponding to approximately 15 polymer repeat units. At 51 wt % liquid crystal (ϕ_{LC} = 0.49), a lamellar morphology is clearly visible. HPL defects can be observed in the upper portion of the micrograph throughout the sample, confirming the SAXS profile discussed earlier (Figure 2). From the micrograph, the lamellar periodicity is approximately 10−12 nm, and the apparent thickness of the LC layer is 3.5−4 nm. The spacings correspond to a LC volume percent of approximately 35−40%, slightly lower than the volume fraction of 49% as determined from GPC data. Lower LC volume fractions are found with most of the TEM micrographs. The polystyrene block consistently has a larger volume fraction as observed in TEM than that predicted from molecular weight and density measurements. This may be a result of staining for the same reasons discussed earlier in the case of cylinders.

As the PS block length is increased, the dark polystyrene regions increase in width, as seen in Figure 5a−c, and the white LC regions maintain a roughly constant width. PS−HBPB41 and PS−HBPB32 appear to have the most well-defined block copolymer interfaces. This is probably due to the effects of increased molecular weight and higher degrees of phase segregation. On the other hand, with increasing PS content, a greater number of defects are present, leading to smaller grain sizes. The same effects just described are also present in the decyl series. A similar series of micrographs in order of increasing polystyrene block length are shown in Figure 6a−c for the decyl series.

In these PS−*n*BPB diblock copolymers, focal−conic fan-shaped superstructures were observed, as described previously.[13] For high LC volume fractions and low molecular weights, as in PS−DBPB63, the copolymer fan grains are one to several microns in size, and one can observe large, onion-shaped, curved lamellae that appear to be focal−conic Dupin cyclides; Figure 6a is a section of such a structure. As the MW increases, and the PS block becomes longer, the grain size decreases from several microns to, at best, tens of nanometers. The drop in grain size with increasing PS content is further evidenced from the room-temperature optical micrographs shown in Figure 7. For these micrographs, all materials were annealed in the smectic C* mesophase; annealing times were 24 h for samples in

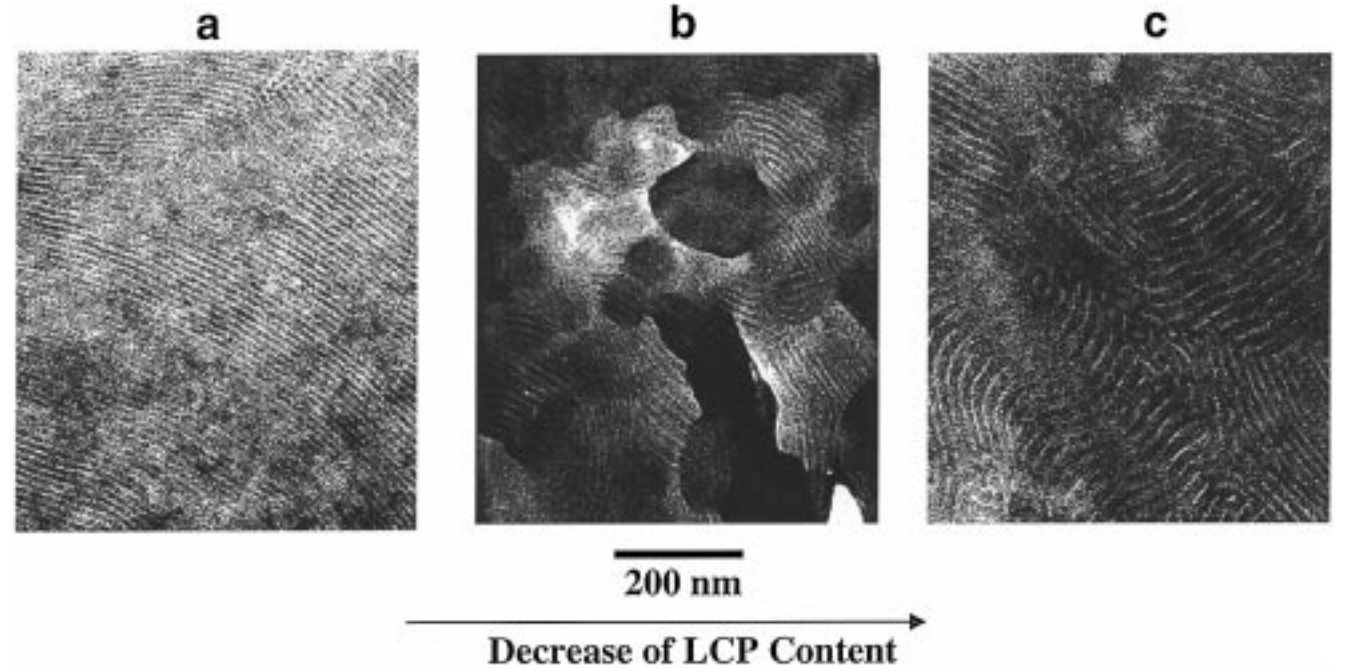

Figure 5. TEM images of PS−HBPB series in order of increasing polystyrene block length and decreasing LC content: (a) PS−HBPB51, $M_n = 14\,300$; (b) PS−HBPB41, $M_n = 18\,300$; (c) PS−HBPB32, $M_n = 19\,100$. Samples were taken from solution-cast films that were annealed for 2 days at 110 °C.

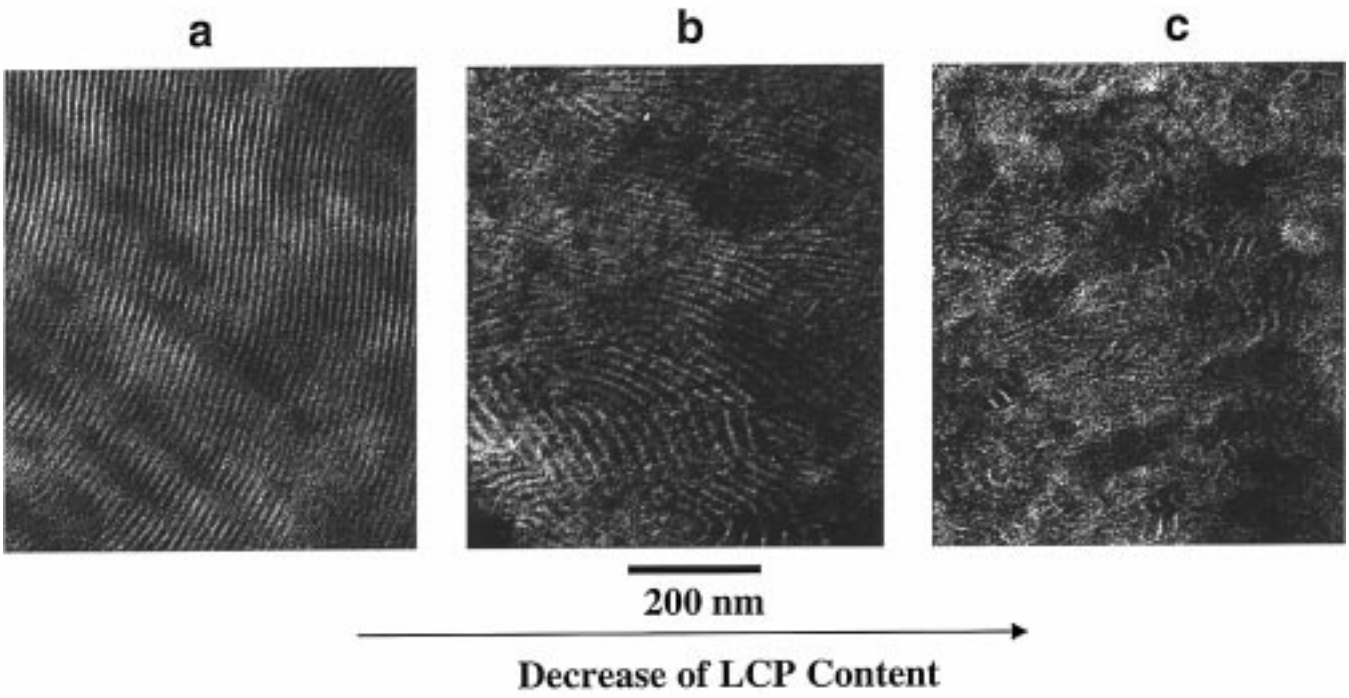

Figure 6. TEM images of PS−DBPB series in order of increasing polystyrene block length and decreasing LC content: (a) PS−DBPB63, $M_n = 14\,400$; (b) PS−DBPB49, $M_n = 19\,000$; (c) PS−DBPB37, $M_n = 22\,600$. Samples were taken from solution-cast films that were annealed for 2 days at 110 °C.

Figure 7b,c to achieve close to equilibrium structures and 1 h for the homopolymer in Figure 7a. At higher PS contents, moving from Figure 7b to 7c and 7d, the grain size shrinks, and the birefringent texture becomes progressively finer and ill-defined. The differences in grain size may be due to kinetic effects in part; higher molecular weight polymers will be more sluggish in achieving LC arrangements. These effects may also be enhanced by the phase behavior of these materials. We have observed that the block copolymer order−disorder transition (ODT) of these materials is coincident with the LC clearing point at low molecular weight but becomes independent of the LC mesophase at higher molecular weights and PS volume fractions.[13] For higher molecular weights, the spontaneous formation of larger superstructures may be inhibited by the presence of existing microphase segregated domains. When block copolymer and LC ordering occur simultaneously, the LC superstructure dominates the formation of micron-sized block copolymer grains.

The degree of incompatibility between the LC and polystyrene phase is weakest in the decyl series. This is apparent if one examines Figures 5 and 6; the decyl diblocks appear to have more diffuse interfaces, and

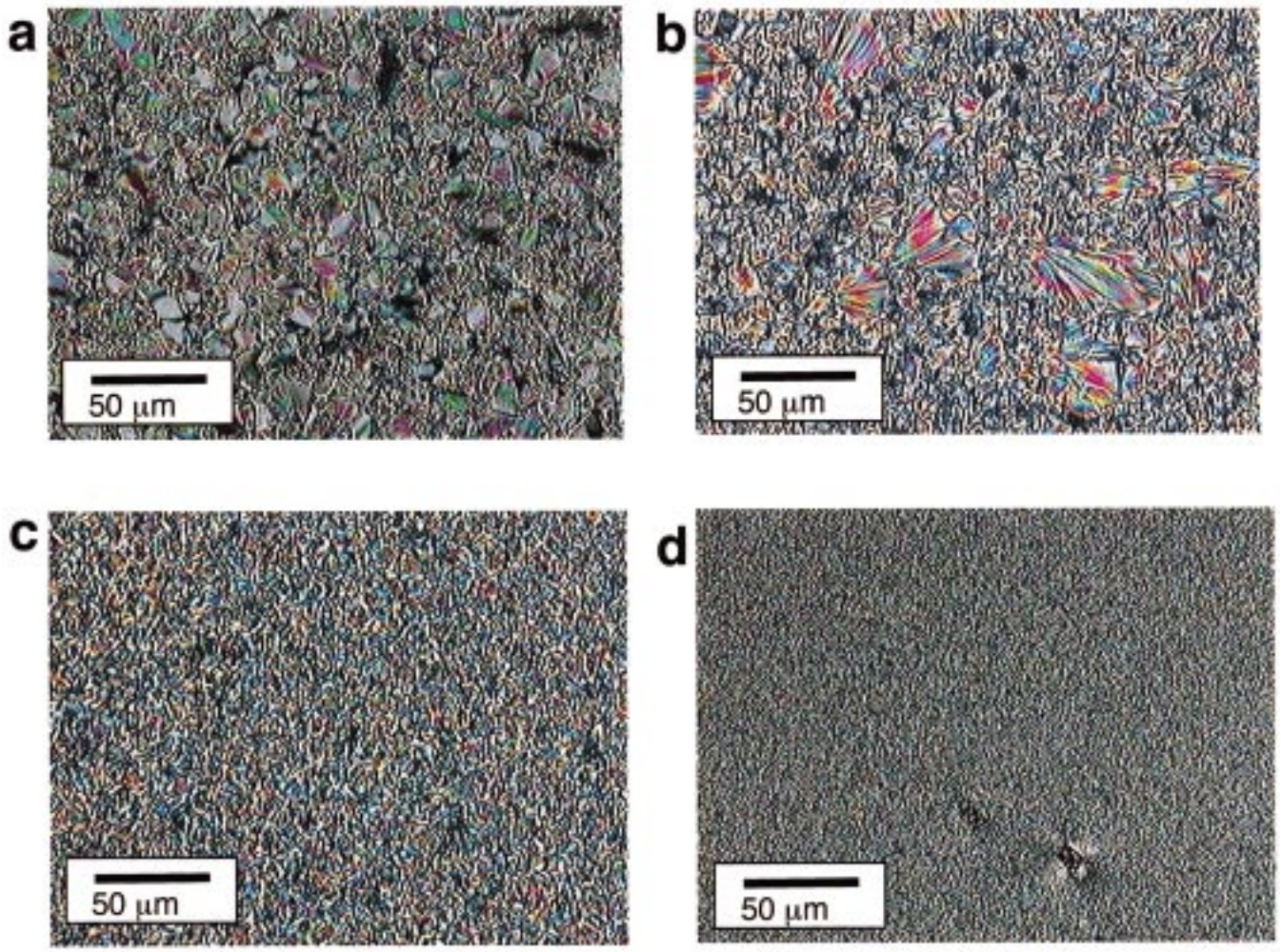

Figure 7. LC textures at room temperature from polarized optical microscopy for DBPB polymers at varying compositions: (a) DBPB homopolymer, $M_n = 8300$; (b) PS−DBPB63, $M_n = 14\,400$; (c) PS−DBPB57, $M_n = 17\,500$; (d) PS−DBPB49, $M_n = 19\,000$.

smaller grain sizes, at 37 wt % ($\phi_{LC} = 0.35$) LC (Figure 6c) than the hexyl does at 32 wt % ($\phi_{LC} = 0.30$) LC (Figure 5c). SAXS confirms this observation—films from the decyl series with low LC contents tend to have weaker SAXS reflections than the hexyl series. These observations could imply that longer alkyl spacers compatibilize the two blocks.

Thus, in summary, by systematically increasing the length of the PS block, a larger number of defects appear in the diblock copolymer microstructure, resulting in smaller grain sizes. Also, diblocks with decyl spacers have a higher degree of phase mixing at the block copolymer interface.

C. Orientation Effects. One of the advantages of block copolymer liquid crystalline systems is the ability to use processing approaches to obtain oriented samples. Shear and flow induced orientation of block copolymer morphologies has been observed in amorphous[29,30] and semicrystalline[31,32] block copolymers. In both cases, orientation was affected by the processing temperature. In this study, samples of both hexyl and decyl series of block copolymers were roll-cast to introduce morphological orientation. Roll-cast films were prepared for diblock copolymers exhibiting predominately lamellar morphology. SAXS was used to examine the arrangement of diblock copolymer morphology and LC smectic layers relative to the flow direction. In all experiments, the X-ray beam was positioned orthogonal to the film plane

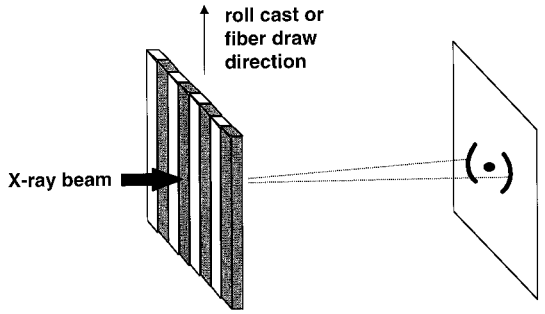

Figure 8. Beam-to-sample orientation in SAXS experiments of roll-cast and fiber-drawn PS−*n*BPB diblocks.

and perpendicular to the roll-casting flow field as shown in Figure 8. TEM micrographs of roll-cast diblock copolymers confirm that lamellar sheets preferentially orient perpendicular to the plane of the film and in the flow direction.

Lamellar Systems. A 2D SAXS diffraction pattern for the roll-cast sample of PS−HBPB54 is shown in Figure 9a. The innermost arcs on the horizon indicate the preferential ordering of the block copolymer microdomains and correspond to a *d* spacing of 169 Å. The arcs are perpendicular to the direction of flow and indicate that the block copolymer lamellae are orthogonal to the flow direction. Only a first-order peak was observed; however, this signal is very broad, and higher-

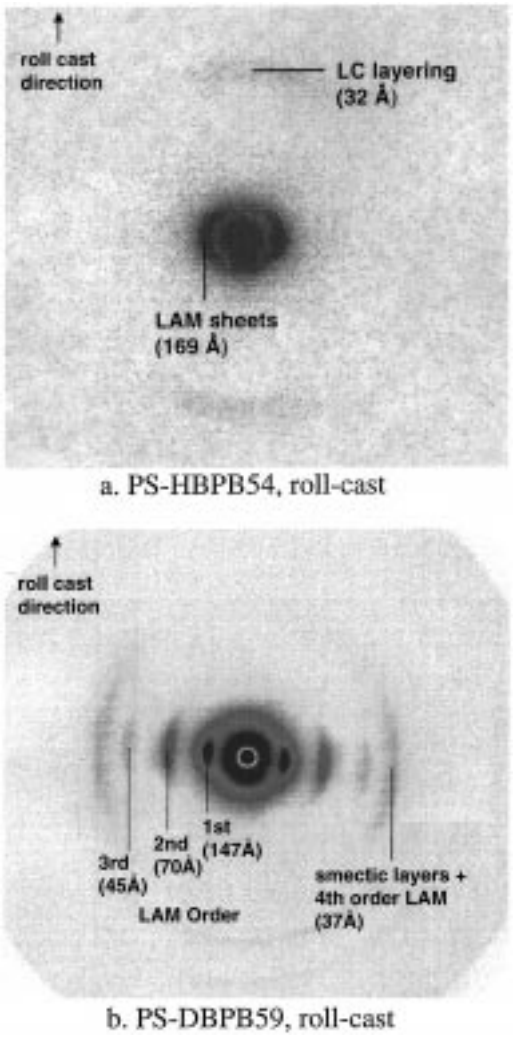

Figure 9. SAXS diffraction patterns of roll-cast samples: (a) PS−HBPB54, (b) PS−DBPB59.

order peaks may be convoluted in the tail of the first-order peak. The first-order SAXS peak in a simple-cast, unoriented specimen corresponds to a spacing of 178 Å, which is somewhat larger than the roll-cast sample reflection (169 Å). Studies of roll-cast block copolymers suggest that a slight decrease in *d* spacing is seen in roll-cast materials due to the deformation of the film.[15,16] A second set of arcs appear at 32 Å on the meridian in Figure 9a, perpendicular to the block copolymer arcs, and are due to alignment of smectic layers. The same sort of Bragg spacing is also observed in the smectic homopolymer. By comparing the position of the morphological and smectic layer reflections, it can be concluded that mesogens orient along the flow direction, to form smectic layers perpendicular to the block copolymer lamellar morphology.

A perpendicular orientation of smectic layers to morphology has also been observed in several other liquid-crystalline diblocks having lamellar morphology.[6,19,33,34] In these cases, the structure of the side chains in the liquid-crystalline block are all somewhat similar. The smectic mesogens consist of conjugated, rodlike systems (e.g., biphenyl, cholesteryl, or azobenzene) separated from the main chain by short, alkyl spacers $-(CH_2)_n-$ where $n = 2-6$. The perpendicular arrangement is thought to be based on the tendency of LC block polymer backbone to extend outward from the copolymer interface; the mesogens will then orient

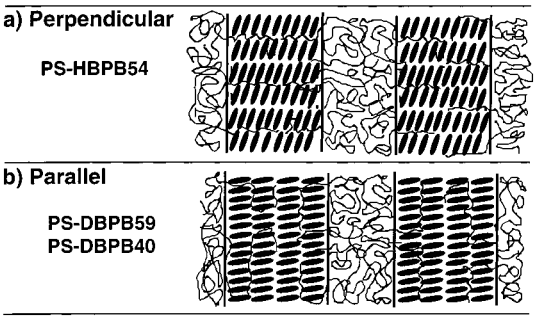

Figure 10. Schematic of relative orientations of mesogens to aligned morphology in roll-cast PS-*n*BPB samples with lamellar morphologies: (a) perpendicular, (b) parallel.

perpendicular to the main chain forming smectic layers perpendicular to the block copolymer interface.[6]

In contrast, a 2D SAXS pattern of a roll-cast block copolymer with a decyl spacer, PS−DBPB59, is shown in Figure 9b. The lowest-angle scattering signals appear as arcs positioned perpendicular to the flow direction at 147 Å, implying that lamellae align in the direction of flow and are perpendicular to the film surface. There are five other peaks in the same direction corresponding to the second- through sixth-order scattering peaks for lamellar morphology. The fourth peak corresponds to a *d* spacing of 37 Å and is unusually large. This peak was shown to be a convolution of the fourth-order reflection from lamellar morphology (39 Å) and a scattering signal from LC smectic layer spacing (32 Å). In conclusion, roll-casting causes smectic layers of PS−DBPB59 to organize parallel to the aligned block copolymer lamellae as indicated by Figure 10b. This arrangement, which is counter to the expected orientation, had not been observed previously and was the subject of a recent communication.[2] A sample with a lower liquid crystal volume fraction, PS−DBPB40, also exhibits parallel orientation of the smectic layers relative to lamellar morphology, confirming the effect of the decyl spacer in this series of copolymers. For PS−DBPB40, a first-order reflection for the block copolymer domains is present at the horizon at 209 Å. The smectic layers reflect in the same plane at 24 Å; this remarkably small smectic layer spacing implies the mesogens likely have a high tilt angle in the oriented film.

The roll-cast films are believed to have near-equilibrium macromolecular structures for both hexyl and decyl samples, due to the use of a neutral solvent and long annealing times. Annealing the roll-cast diblocks at 80 °C for 24 h usually had no further effect on the orientation and, in some cases, even increased the intensity of diffraction in SAXS. It is interesting to note that the transitional morphologies seen in bulk, simple cast films are not present in the roll-cast samples. Perforated or modified layer defects are no longer apparent in the TEM micrographs, and SAXS generally indicates single primary peaks for all samples. It is likely that the transitional morphologies observed in simple cast annealed films reflect metastable arrangements or arrangements that may be kinetically hindered during the room temperature solvent evaporation process used for the roll-cast systems.

For these two very similar LC block copolmer systems, we thus have two differing preferred forms of orientation, as shown in Figure 10. The perpendicular arrangements of smectic layers within block copolymer lamellae in the hexyl systems appear to be consistent with the

concept of a more fully extended polymer main chain, from which mesogens dangle to form layers and anchor with their lengths along the interface. However, the added alkyl length in the decyl series appears to lead to parallel smectic layers in which the mesogens anchor with their lengths perpendicular to the surface and their tail groups at the interface. This arrangement might be allowed due to the added conformational freedom of the mesogen, which is more decoupled from the main chain than the hexyl polymers. In general, the minimization of free energy at the block copolymer interface, or other anchoring effects, may induce homeotropic or parallel arrangements of smectic layers without the constraints of the polymer main chain. The interfacial tension between the two blocks may present an anchoring effect within microphase segregated domains, which, in the absence of a polymer backbone, would lead to a parallel arrangement of smectic layers. Also, if one considers the mesogen−mesogen interactions, this orientation is preferred, as the number of lateral interactions are maximized when the mesogens orient orthogonal to the planar boundaries.

To determine the impact of fiber-drawing on morphological and liquid-crystal orientation, the following lamellar block copolymers were fiber-drawn at temperatures close to the clearing point: PS−DBPB59, PS−DBPB33, and PS−DBPB40. Generally, the morphology in fiber-drawn samples was found to be more highly aligned than roll-cast samples due to the high degree of extension during the drawing process. Reflection arcs appear more intense, and there is less scattering in regions between the arcs, indicating a higher-order parameter. Morphological domain sizes were consistently observed to be smaller in fiber-drawn samples compared to unoriented or roll-cast samples due to mechanical orientation effects. All fiber-drawn samples of the LC diblocks with decyl spacers show smectic layers are oriented perpendicular to both the fiber axis and the aligned lamellar domains, yielding diffraction patterns analogous to Figure 9a. This is a surprising result because it is the opposite of that observed in the roll-cast films of the same copolymers; roll-cast films are closest to equilibrium due to the slow rate of solvent removal and, in some cases, subsequent annealing. These differences may well be due to the effect of the large tensile shear forces produced in the bulk melt phase when drawing fibers and the fact that the block domains and the individual mesogens both act as mechanical elements which respond by alignment in this shear field. Tokita et al. found liquid-crystalline homopolymers to orient with lamellar smectic layers parallel to the direction of stress in fibers drawn from the LC state but with smectic layers perpendicular to stress if drawn from the isotropic state.[35] The roll-casting process, on the other hand, presents normal shear forces, lower in magnitude, to a polymer solution undergoing a slow, controlled solidification. This second situation results in the orientation of the block copolymer morphology, within which a near-equilibrium rearrangement and anchoring of the smectic layers within the oriented domain takes place.

Cylinders. We have also investigated orientation effects in cylindrical morphologies. As mentioned above, the PS−HBPB79 sample consists of polystyrene cylinders in an LC matrix. A sample of PS−HBPB79 was roll-cast and examined using SAXS. The resulting diffractogram is shown in Figure 11a, and the pattern

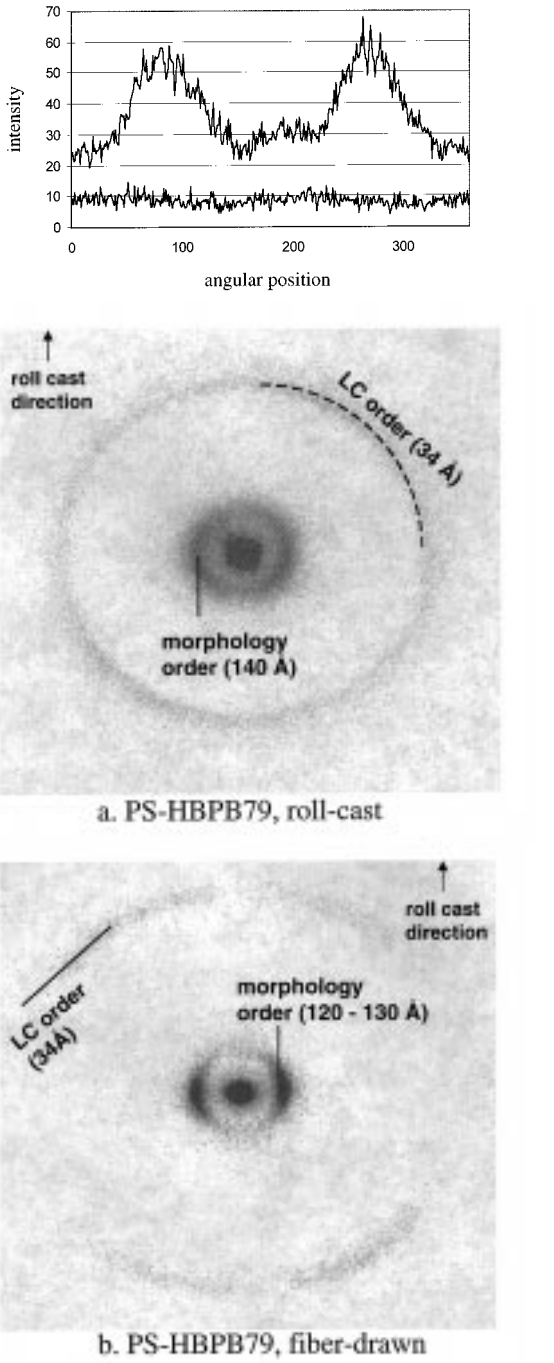

Figure 11. SAXS diffraction patterns of oriented PS−HBPB79 exhibiting cylindrical morphologies: (a) roll-cast, (b) fiber-drawn. The inset in (a) includes plots of intensity vs angular position obtained from a 2θ integration over two isolated rings. The upper curve represents intensity integrated from $q = 0.43$ to 0.57 nm^{-1} and shows orientation of the cylindrical morphology. The lower curve includes intensity integrated between $q = 1.78$ and 2.06 nm^{-1} and shows the lack of smectic layer orientation.

shows a reflection band at 140 Å. The primary reflections appear on the horizon as two diffuse, low-angle arcs that indicate a weak preferential ordering of block copolymer microdomains perpendicular to the flow direction. Only a broad first-order peak was observed, and cylindrical morphology could not be confirmed on the basis of higher-order peaks; however, the position of the morphology reflections in the 1D curve are very similar to that observed in the simple-cast. Another major reflection appears at 34 Å due to the LC smectic

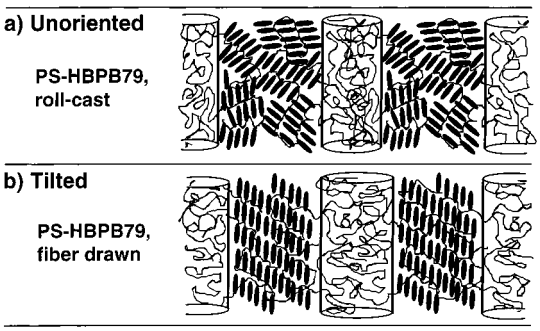

Figure 12. Schematic of relative orientations of mesogens to aligned morphology in PS−HBP79: (a) unoriented (roll-cast), (b) tilted (fiber-drawn).

layers. This reflection consists of a circle with nearly uniform intensity. The absence of arcs indicates smectic layers form without a preferred direction; this may be due to the relatively poor alignment of the cylindrical morphology. Fischer observed that a parallel orientation of smectic layers may be found in cylindrical or spherical morphologies with a continuous LC phase.[34]

PS−HBPB79 was also fiber-drawn and annealed for 24 h at 80 °C. The resulting SAXS pattern is shown in Figure 11b. The inner two arcs correspond to a *d* spacing around 120−130 Å and indicate that the block copolymer cylinders are oriented in the flow direction. At wider angles the smectic layer reflections display four maxima, each tilted about 50°−60° with respect to the aligned cylinders. The predicted LC organization for this system is shown in Figure 12b. The smectic layers are believed to assume a tilted orientation with respect to the PS cylinders (∼50°−60°). This angle should not be confused with the smectic C* mesogen tilt angle, which is the angle between the mesogen director and the smectic layer normal. On the basis of the analysis of wider-angle X-ray patterns which are not shown here, the smectic C* tilt angle is estimated to be about 30°. Considering these observations, both the PS cylinders and the LC mesogens are believed to align in the direction of flow, making the LC superstructure in Figure 12b plausible. The observed phenomenon is comparable to that described by Quiram and Register in the study of the polyethylene chain folding direction in semicrystalline asymmetric block copolymers.[36] Here, crystallizable polyethylene was confined to strongly segregated block copolymer cylindrical microdomains, and in fast-cooled samples, the polyethylene chain axis was found to be preferentially tilted with respect to the cylindrical morphology, just as the smectic layers are angled with respect to the cylinders in the PS−HBPB79 fiber-drawn sample.

Conclusions

In this paper, using results of SAXS and TEM experiments, the interplay between liquid crystallinity and microphase segregated morphologies in a series of PS−*n*BPB diblock copolymers has been addressed. Smectic layering in the liquid-crystalline subphase appears to stabilize lamellar morphologies, as evidenced by an unusually broad lamellar regime; these observations are consistent with those of earlier researchers.[19−21] The lamellar region of the phase diagram is asymmetric; there are indications of continuous LC phases, in the form of ML and HPL defects, at unusually low LC volume fractions starting at $\phi_{LC} = 0.50$. The observations of these phases suggests that the arrangement of the LC phase, and/or the presence of the large bulky side groups, significantly influence the curvature of the block copolymer interface. In the lamellar regime, with increasing PS block length, at constant LC block length, both the morphological grain size and the liquid-crystal defect size decrease 2−3 orders of magnitude. These effects are thought to be due to a combination of kinetic effects with increasing molecular weight and, more importantly, the influence of the LC on the ordering of the block copolymer with changing volume fraction. This information may prove crucial in applications where the formation of a large monodomain is necessary.

Orientation studies of these materials indicate ordering of the LC phase within the block copolymer is a function of the length of the alkyl spacer. Hexyl spacer systems orient with the smectic layers perpendicular to the block copolymer lamellae; however, decyl spacer systems orient with the smectic layers parallel to the lamellae. These observations, which have not been observed in other LC block copolymer systems, are thought to be due to differences in the degree of decoupling of the mesogen from the polymer main chain conformation. This observation, combined with surface tension and thermodynamic considerations, indicates that, in the absence of a polymer chain, the BPB mesogen prefers to orient homeotropically with respect to the block copolymer interface. In melt-drawn fibers, both the LC element and the morphology respond to shear, resulting in perpendicular arrangements. Finally, a block copolymer with a morphology of PS cylinders in an LC matrix exhibited poorly oriented LC domains when roll-cast, but when fiber-drawn, it was found that the LC layers were tilted 50°−60° with respect to aligned morphology.

References and Notes

(1) Mao, G.; Wang, J.; Ober, C. K.; O'Rourke, M. J.; Thomas, E. L.; Brehmer, M.; Zentel, R. *Polym. Prepr.* **1997**, *38*, 374−375.
(2) Zheng, W. Y.; Albalak, R.; Hammond, P. T. *Macromolecules* **1998**, *31*, 2686−2689.
(3) Adams, J.; Gronski, W. *Makromol. Chem., Rapid Commun.* **1989**, *10*, 553−557.
(4) Zaschke, B.; Frank, W.; Fischer, H.; Schmutzler, K.; Arnold, M. *Polym. Bull.* **1991**, *27*, 1−8.
(5) Bohnert, R.; Finkelmann, H. *Macromol. Chem. Phys.* **1994**, *195*, 689−700. Chiellini, E.; Galli, G.; Angeloni, S.; Laus, M. *Macromol. Symp.* **1994**, *77*, 349−358.
(6) Yamada, M.; Iguchi, T.; Hirao, A.; Nakahama, S.; Watanabe, J. *Macromolecules* **1995**, *28*, 50−58.
(7) Fischer, H.; Poser, S. *Acta Polym.* **1996**, *47*, 413−428.
(8) Zheng, W. Y.; Hammond, P. T. *Macromol. Rapid Commun.* **1996**, *17*, 813−824.
(9) Omenat, A.; Hikmet, R. A. M.; Lub, J.; van der Sluis, P. *Macromolecules* **1996**, *29*, 6730−6736.
(10) Mao, G.; Wang, J.; Ober, C. K.; Brehmer, M.; O'Rourke, M. J.; Thomas, E. L. *Chem. Mater.* **1998**, *10*, 1538−1545.
(11) Brehmer, M.; Mao, G.; Ober, C. K. *Macromol. Symp.* **1997**, *117*, 175−179.
(12) Zheng, W. Y.; Hammond, P. T. *Side Chain Liquid Crystalline Block Copolymers with Chiral Smectic C Mesogens*; Bunning, T. J., Hawthorne, S. H. C. W., Koide, N., Kajiyama, T., Eds.; MRS Symposium Proceedings: San Francisco, 1996; Vol. 425.
(13) Zheng, W. Y.; Hammond, P. T. *Macromolecules* **1998**, *31*, 711−721.
(14) Zheng, W. Y.; Hammond, P. T. *Synthesis and Characterization of Block Copolymers with Smectic C* Liquid Crystalline Mesogens*: Miami, 1995.
(15) Albalak, R. J.; Thomas, E. L. *J. Polym. Sci., Polym. Phys. Ed.* **1994**, *32*, 341.
(16) Albalak, R. J.; Thomas, E. L. *J. Polym. Sci., Polym. Phys. Ed.* **1993**, *31*, 37.
(17) Lednicky, F. *Collect. Czech. Chem. Commun.* **1995**, *60*, 1935−1940.
(18) Koizumi, S.; Hasegawa, H.; Hashimoto, T. *Macromolecules* **1994**, *27*, 6532−6540.

(19) Mao, G.; Wang, J.; Clingman, S. R.; Ober, K.; Chen, J. T.; Thomas, E. L. *Macromolecules* **1997**, *30*, 2556−2567.
(20) Fischer, H.; Poser, S.; Arnold, M.; Frank, W. *Macromolecules* **1994**, *27*, 7, 7133−7138.
(21) Fischer, H.; Poser, S.; Arnold, M. *Liq. Cryst.* **1995**, *18*, 503−509.
(22) Yamada, M.; Itoh, T.; Nakagawa, R.; Hirao, A.; Nakahama, S.; Watanabe, J. *Macrmolecules* **1999**, *32*, 282−289.
(23) Hajduk, D. A.; Gruner, S. M.; Rangarajan, P.; Register, R. A.; Fetters, L. J.; Honeker, C.; Albalak, R. J.; Thomas, E. L. *Macromolecules* **1994**, *27*, 490−501.
(24) Hamley, I. W.; Koppi, K. A.; Rosedale, J. H.; Bates, F. S.; Almdal, K.; Mortensen, K. *Macromolecules* **1993**, *26*, 5959−5970.
(25) Hamley, I. W.; Gehlsen, M. D.; Khandpur, A. K.; Koppi, K. A.; Rosedale, J. H.; Schulz, M. F.; Bates, F. S.; Almdal, K.; Mortensen, K. *J. Phys. II* **1994**, *4*, 2161−2186.
(26) Heck, B.; Arends, P.; Ganter, M.; Kressler, J.; Stuehn, B. *Macromolecules* **1997**, *30*, 4559−4566.
(27) Fischer, H. *Macromol. Rapid. Commun.* **1994**, *15*, 949−953.
(28) Gido, S. P.; Wang, Z. G. *Macromolecules* **1997**, *30*, 1997.
(29) Koppi, K. A.; Tirrell, M.; Bates, F. S.; Almdal, K.; Colby, R. H. *J. Phys. II* **1992**, *2*, 1941.
(30) Tepe, T.; Schulz, M. F.; Zhao, J.; Tirrell, M.; Bates, F. S. *Macromolecules* **1995**, *28*, 3008−3011.
(31) Kofinas, P.; Cohen, R. E. *Macromolecules* **1994**, *27*, 3002−3008.
(32) Kofinas, P.; Cohen, R. E. *Macromolecules* **1995**, *28*, 336−343.
(33) Adams, J., Gronski, W., Weiss, R. A. O., C. K., Eds.; American Chemical Society: Miami Beach, FL, 1996; pp 174−184.
(34) Fischer, H.; Poser, S.; Arnold, M. *Macromolecules* **1995**, *28*, 6957−6962.
(35) Tokita, M.; Osada, K.; Kawauchi, S.; Watanabe, J. *Polym. J.* **1998**, *30*, 687−690.
(36) Quirem, D. J.; Register, R. A.; Marchand, G. R. *Macromolecules* **1997**, *30*, 4551−4558.

MA9903153